

Eliashberg function $\alpha^2F(\omega)$ and phonon spectrum $F(\omega)$. A simple model for an amorphous s - p superconductor

S. J. Poon and T. H. Geballe

Department of Applied Physics, Stanford University, Stanford, California 94305

(Received 16 January 1978)

A simple expression of the Eliashberg function $\alpha^2F(\omega)$ for an amorphous s - p superconductor is obtained. One finds that $\alpha^2F(\omega) = (1/\omega)\sum_q [L(\vec{q}) + N(\vec{q})]\delta(\omega - \omega_q)$, where \vec{q} includes the phonon branch index; $N(\vec{q})/\omega_q$ is the N process which conserves "lattice" momentum; $L(\vec{q})/\omega_q$ replaces the U process in the crystalline phase and it selects "lattice" momentum through the structure factor of the amorphous phase. Both $L(\vec{q})$ and $N(\vec{q})$ are evaluated using the Heine-Animalu pseudopotential form factor and experimental structure factor. A qualitative deconvolution of the phonon spectrum $F(\omega)$ from $\alpha^2F(\omega)$ for four alloys is attempted. The main findings are: (i) Due to the nonconservation of "lattice" momentum in the conventional sense, $\alpha^2F(\omega)$ depends linearly on ω in the low- ω region, similar to Bergmann's results on disordered superconductors. The calculated first derivatives of $\alpha^2F(\omega)$ are in good agreement with tunneling data on amorphous superconductors. (ii) The deconvoluted $F(\omega)$ are in better agreement with theoretical results obtained using the Morse potential than the Lennard-Jones potential. (iii) The Hopfield-McMillan parameter η tends to decrease in the amorphous phase. Results (ii) and (iii) are discussed in terms of structural short-range order in the amorphous state. For the purpose of comparison, a similar calculation is made for crystalline Pb; it is found that there is no unambiguous enhanced $\alpha^2F(\omega)$ in the low- ω region.

I. INTRODUCTION

So far there have been more experimental results than theoretical treatment in the field of amorphous superconductors.¹ Within the Eliashberg theory of strong-coupling superconductors,^{2,3} the parameters which determine the superconducting transition temperature T_c are the electron-phonon spectral function (or the Eliashberg function) $\alpha^2F(\omega)$ and the Coulomb pseudopotential μ^* . One can determine both quantities from tunneling experiments on amorphous superconductors assuming that the Eliashberg theory can be applied to a disordered matrix. To be able to extract microscopic information on the electron-phonon interaction from experimental results, one almost has to perform a first-principles calculation on certain relevant parameters such as band structure, pseudopotential, phonon dispersion, etc. Such can be done for the crystalline state where the electronic and vibrational eigenstates are known. Meanwhile, similar attempts^{1,4} have also been made on amorphous superconductors where both eigenstates are least known. The common result of these latter investigations is that there is an enhanced electron-phonon interaction at low energy which leads to the strong-coupling behavior in these materials. The enhancement is due to either the presence of additional low-energy phonons or an enhanced electron-phonon coupling. Thus information on the phonon spectrum $F(\omega)$ would allow a comparison with experimental results on $\alpha^2F(\omega)$. In crystalline materials, there

is a rather close similarity between the two spectra.⁵ So far only theoretical results on $F(\omega)$ of model amorphous structure are available.⁶⁻⁸ By considering the effect of topological disorder alone, von Heimendahl and Thorpe⁶ concluded that the vibrational density of states in amorphous metals should be similar to those of fcc and hcp metals. More recent calculations^{7,8} on tight-binding "Lennard-Jones glass" in which both topological and quantitative (those related to bonding forces) disorder are treated show essentially featureless density of states.

While there are no $\alpha^2F(\omega)$ data on amorphous d -band superconductors, those on s - p metals are available. Up to this point, inelastic-neutron-scattering data on both s - p and d -band amorphous metals do not exist in the literature. Tunneling results on amorphous s - p metals¹ reveal spectra consisting of distinct longitudinal features despite an overall smearing of the phonon modes. However, there is no *a priori* reason to assume a close similarity between $F(\omega)$ and $\alpha^2F(\omega)$ in amorphous metals. On the other hand, studies of elastic properties of glassy metals⁹ indicate a significant decrease in the shear modulus with respect to the crystalline state while the bulk modulus is essentially unchanged. Bolz and Pobel¹⁰ observed almost the same value of $\int_0^\infty [F(\omega)/\omega]d\omega$ in both crystalline and amorphous Sn. These facts suggest that the "characteristic" energy of the phonon spectrum might be insensitive to disorder. In this paper, we attempt to deconvolute $F(\omega)$ from $\alpha^2F(\omega)$ data on amorphous s - p superconductors.

Our results reveal a distinct density of states of longitudinal modes in *s-p* amorphous metals.

We derive a simple expression of $\alpha^2 F(\omega)$ for amorphous *s-p* superconductors using the pseudopotential theory. The expression depends on the phonon frequency ω_q , the structure factor $A(K)$, and the pseudopotential form factor V_Q . Deconvolution of $F(\omega)$ from $\alpha^2 F(\omega)$ is attempted by using quadratic phonon dispersion curves and also taking into account uncertainties in \vec{q} . Comparison of $\alpha^2 F(\omega)$ with experiments is made for the low- ω region. The effects of absence of long-range order on the Hopfield-McMillan atomic parameter η and transition temperature T_c are discussed. A comment is made on the relationship between amorphous and strong-coupling behavior in amorphous *s-p* superconductors. Finally, for comparison purposes, similar calculations are done for crystalline Pb. The plan of this paper is as follows: in Sec. II A an expression of $\alpha^2 F(\omega)$ is derived. Section II B presents the properties of the integral $L(\vec{q})$ which is a multiplier in the $\alpha^2 F(\omega)$ expression. Section II C compares our results with experiments in the low- ω region. Section III discusses the relationship between amorphousness, phonon spectrum $F(\omega)$, and other parameters in the superconductivity theory. Section IV presents a calculation on crystalline Pb. Sec. V is the summary and conclusion. The Appendix treats electron-ion interaction in second-order perturbation.

II. $\alpha^2 F(\omega)$ IN AMORPHOUS *s-p* METALS

In this section, we derive an expression of $\alpha^2 F(\omega)$ in close resemblance to the phonon spectrum $F(\omega) = \sum_q \delta(\omega - \omega_q)$ through a multiplier $[L(\vec{q}) + N(\vec{q})]/\omega_q$ in the summation, where q includes the phonon-branch index. It has always been equally difficult to associate a wave vector \vec{q} with a phonon energy ω and a wave vector \vec{k} with an electronic eigenstate $|E\rangle$ in an amorphous metal, since at first sight these wave numbers are not well defined. Despite these drawbacks, it is not impossible to tackle the problem of electron-phonon interaction in an amorphous metal by considering the following points. First, it is unlikely that the uncertainty in \vec{q} in the absence of periodicity can be much larger than some characteristic wave vector, say the Debye wave vector \vec{q}_D , since the sum over phase space give the total number of phonon modes $3N$ (N is the number of atoms in the solid). Second, low-temperature specific-heat experiments on amorphous metals¹ indicate that the main contribution to the lattice specific heat obeys the T^3 law. The Debye temperatures determined from these measurements are lower in

the amorphous phases than in their crystalline counterparts. Thus, at least the density of states (also the \vec{q} - ω relation) of the low-lying acoustical modes obeys the Debye law, with appreciable softening in the transverse modes. In fact, theoretical results¹¹ of longitudinal $\omega(\vec{q})$ for amorphous solids reflect features observed in the crystalline solid. Therefore, it might not be unreasonable to define an "equivalent" dispersion relation for each phonon branch. This approximation enters only when we attempt to deconvolute the phonon spectrum $F(\omega)$ from the Eliashberg function $\alpha^2 F(\omega)$. Uncertainty in $F(\omega)$ due to uncertainty in \vec{q} will be represented by error bars in the figures. It will be shown that the general features of $F(\omega)$ are indeed maintained in the presence of uncertainty in \vec{q} .

The exact electron eigenfunctions in an amorphous solid must have very complicated forms. In *s-p* metals where the pseudopotential theory is well established, one rather takes a perturbative approach using plane waves. It has been shown that^{1,12} such approach accounts for rather well the transport (e.g., Hall effect and resistivity) and optical properties of amorphous and liquid *s-p* metals. These materials are similar from a structural point of view. Similar to previous calculations,¹² we will treat the electron-phonon interaction in amorphous metals using pseudopotentials. The agreement of our calculation with experimental values on $\alpha^2 F(\omega)$ in the low- ω region will be demonstrated. However, one must be cautious in interpreting the tunneling results $\{\mu^*, \alpha^2 F(\omega)\}$ using the aforementioned approach. Besides the normal Coulomb interaction between electrons, the nonphonon parameter μ^* should also include Coulomb scattering of electrons in the static inhomogeneous matrix. The latter determines properties such as resistivity and band structure.

A. The model

The well-known Eliashberg function $\alpha^2 F(\omega)$ is defined as^{13,14}

$$\alpha^2 F(\omega) = \sum_{kk'q} g_{kk'q}^2 \delta(\omega - \omega_q) \delta(\epsilon_k) \delta(\epsilon_{k'}) / \sum_k \delta(\epsilon_k), \quad (1)$$

where $N(0)$ is the single-spin density of states, $g_{kk'q}$ is the electron-phonon coupling matrix element, and the δ functions restrict the electronic states to the Fermi surface. $g_{kk'q}$ is given in the rigid-ion approximation¹⁵ by (see Appendix for the perturbative treatment of *e-p* interaction),

$$g_{kk'q} = \sum_l \left(\frac{\hbar}{2MN\omega_q} \right)^{1/2} e^{i(\vec{k}' - \vec{k} + \vec{q}) \cdot \vec{R}_l} i(\vec{k}' - \vec{k}) \cdot \vec{\epsilon}_q V_{k',k}, \quad (2)$$

where \vec{R}_l denotes the atomic position at site l , $\vec{\epsilon}_q$ is the phonon polarization vector, and $V_{k',k}$ is the Fourier transform of the atomic pseudopotential (the potential which is properly screened) also called the pseudopotential form factor. In a crystalline solid, the lattice sum vanishes unless $\vec{k}' - \vec{k} + \vec{q} = 0$ or \vec{G} , the reciprocal-lattice vector. The former is called the N (normal) process and the latter the U (umklapp) process. The U process depends on periodicity. Thus except for the N process, the selection rules for the U process in an amorphous solid are replaced by a structure factor $A(K)$ defined as

$$A(K) = \frac{1}{N} \sum_{l,l'} \exp[i\vec{K} \cdot (\vec{R}_l - \vec{R}_{l'})] - N\delta_{K,0}. \quad (3)$$

The relationship between \vec{k} , \vec{k}' , and \vec{q} then comes from $A(K)$ through $\vec{K} = \vec{k}' - \vec{k} + \vec{q}$. $A(K)$ is the detected x-ray intensity normalized by the scattering factor. The detected intensity has been corrected for absorption, polarization, multiple scattering, and background. In a well ordered crystalline solid, $A(K)$ contains sharp peaks at the reciprocal lattice vectors \vec{G} which give the partial selection rules for electron phonon interaction. In highly disordered and amorphous solids, a typical $A(K)$ contains a maximum at K_0 , where $K_0 d \approx 7-8$ (d corresponds to the distance between nearest neighbors) and oscillations at higher K which are characteristic of the loss in structural long-range order.¹⁶ This structure factor is connected to the correlation function $\rho(r)$ by a simple relation

$$A(K) = 1 + \int_0^\infty 4\pi r^2 [\rho(r) - \rho_0] \frac{\sin Kr}{Kr} dr, \quad (4)$$

where ρ_0 is the mean density of the solid. In terms of these quantities, the square of the electron-phonon coupling matrix element $g_{kk',q}^2$ is then given by

$$g_{kk',q}^2 = \frac{\hbar}{2MN\omega_q} [A(|\vec{k}' - \vec{k} + \vec{q}|) \times |\vec{\epsilon}_q \cdot (\vec{k}' - \vec{k})|^2 V_{k',k}^2 + N |\vec{\epsilon}_q \cdot \vec{q}|^2 V_q^2]. \quad (5)$$

Putting (5) in (1) gives a general expression of $\alpha^2 F(\omega)$,

$$\alpha^2 F(\omega) = \sum_q \left(\frac{L(\vec{q}) + N(\vec{q})}{\omega} \right) \delta(\omega - \omega_q), \quad (6a)$$

with

$$L(q) = \left(\frac{\hbar}{2MN} \right) \sum_{kk'} A(|\vec{k}' - \vec{k} + \vec{q}|) |\vec{\epsilon}_q \cdot (\vec{k}' - \vec{k})|^2 \times V_{k',k}^2 \delta(\epsilon_k) \delta(\epsilon_{k'}) \left(\sum_k \delta(\epsilon_k) \right)^{-1}, \quad (6b)$$

$$N(q) = \left(\frac{\hbar}{2M} \right) \sum_k |\vec{\epsilon}_q \cdot \vec{q}|^2 V_q^2 \delta(\epsilon_k) \delta(\epsilon_{k+q}) / \sum_k \delta(\epsilon_k). \quad (6c)$$

For the $L(\vec{q})$ term, the constraints on \vec{k} and \vec{k}' come from the structure factor $A(|\vec{k}' - \vec{k} + \vec{q}|)$ and their restrictions to the Fermi surface ($\omega_q \ll \epsilon_F$). The $N(\vec{q})$ term only couples to longitudinal phonons. One can see at once that at low ω (corresponding to low $|\vec{q}|$), $L(\vec{q})$ does not vanish because of the form of $A(K)$. The broadening of $A(K)$ in K space due to structural disorder results in the nonconservation of lattice momentum in the scattering process so that the allowed phase space for \vec{k} to scatter into \vec{k}' is expanded. Thus, there are additional electron-phonon scattering processes which contribute to a nonvanishing $L(\vec{q})$ for low-energy transfer. This conclusion is in agreement with Bergmann⁴ who had studied the Eliashberg function in disordered superconductors by using a structural model in which the displacements of the atoms from their positions in a corresponding crystal are described by a Gaussian distribution. Using a momentum conserving and non-Umklapp electron-phonon interaction Hamiltonian, Keck and Schmid¹⁷ studied the electron-phonon interaction in a metal containing dilute nonmagnetic impurities. By linearizing the correction terms in the electron self-energy, they obtained explicit expressions for phonon emission and absorption processes. They found a linear part [i.e., $\alpha^2 F(\omega) \sim \omega$] shifted by an energy of ~ 1 meV when their results were extrapolated to the very short mean-free-path case in an amorphous metal.

One should also compare expression (6) to a result obtained by Allen.¹⁴ Allen derived $\alpha^2 F(\omega)$ in the form $\alpha^2 F(\omega) = [2/\pi N(0)\omega] \sum_q \gamma_q \delta(\omega - \omega_q)$, where γ_q is the intrinsic phonon linewidth. Thus, the quantity $L(\vec{q}) + N(\vec{q})$ can be related to γ_q by $L(\vec{q}) + N(\vec{q}) = [2/\pi N(0)] \gamma_q$. Theoretically, one should then be able to calculate the linewidth of phonons in an amorphous solid. In Sec. II B, we shall exploit the properties of $L(\vec{q})$ to give further insight into the problem of electron-phonon interaction in an amorphous superconductors.

B. Properties of $L(\vec{q})$

By using a spherical phonon model so that $L(\vec{q}) = L(q)$ and taking $\vec{\epsilon}_q$ as purely longitudinal or transverse, (6b) is reduced to

$$L(q) = \frac{\hbar N(0)}{12MNk_F^2} \int_0^{2k_F} dQ \int_{-1}^1 dx f(x) A(|\vec{Q} + \vec{q}|) Q^3 V_Q^2, \quad (7)$$

for each branch, with $\vec{Q} = \vec{k}' - \vec{k}$. The function $f(x) = \frac{1}{2}x^2$ and $\frac{1}{4}(1-x^2)$ for the longitudinal and trans-

verse modes, respectively, where $x = \vec{q} \cdot \vec{Q} / |\vec{q} \cdot \vec{Q}|$. $L(q)$ can be evaluated knowing the experimental structure factor $A(K)$ and the pseudopotential form factor V_Q . $N(\vec{q})$ is evaluated by setting $\vec{G} = 0$ in (13) of Sec. IV. One should notice that $L(0) \propto \rho$, the electrical resistivity of the metal in the Ziman theory for liquid metals.¹⁸ In fact, by rearranging the quantities in $L(0)$ and ρ , one obtains

$$L(0) = [2e^2 E_F k_F^2 N(0) / 9\pi m M N V] \rho. \quad (8)$$

One should note that $L_l(0) = L_t(0) = L(0)$. Another limiting value of $L(q)$ is noted when $q \rightarrow \infty$. The structure factor tends to unity at large $|\vec{Q} + \vec{q}|$ and so $L(\infty) \propto \int_0^{2k_F} Q^3 V_Q^2 dQ$ which is recognized as the integral determining the Hopfield-McMillan parameter η_{xtal} in the crystalline state.¹³ From (7)

$$L(\infty) = \hbar \eta_{\text{xtal}} / 6MN, \quad (9)$$

with $L_l(\infty) = L_t(\infty) = L(\infty)$. For the intermediate values of $L(q)$ one has to know $A(K)$ and V_Q . For the discussion on $F(\omega)$ in the next section, we have chosen to evaluate $L(q)$ for four amorphous alloys whose phonon density of states in the elemental crystals are well studied. These systems are $\text{In}_{80}\text{Sb}_{20}$, $\text{Sn}_{90}\text{Cu}_{10}$, $\text{Pb}_{90}\text{Cu}_{10}$, and $\text{Tl}(+\text{Te})$. It should be reminded that the discussion so far involves only elemental amorphous metals. However, it is not difficult to generalize the present model to binary alloys, especially when the B elements play only a minor role on the superconductive properties. For example, Drierach *et al.*¹⁹ have extended the Ziman theory for liquid metals to binary systems.

For the present study, we have used the Animalu-Henle²⁰ model pseudopotential form factors of the four elements In, Sn, Pb, and Tl. On the other hand, structure factors for these systems are not known. We have chosen the structure factors of the corresponding liquid metals. To minimize the discrepancies between the amorphous and liquid structures, we have adopted the procedure of extrapolating the literature $A(K)$ at temperature T in the liquid state to $T = 0$ by including

a temperature damping factor as outlined by Andonov²¹ for the Pd-Si alloys. For the latter system, small discrepancies between the $A(K)$ in the amorphous state extrapolated to high temperature and that in the liquid state still exist. But such minor discrepancies should not affect our results. One can also undertake a "model" approach of simulating $A(K)$ for these binary systems by using the Percus-Yevick hard-sphere model.²² Knowing the hard-sphere diameters and the packing fraction from the "dense-random-packing" model,¹⁶ one then obtains the partial structure factors needed to calculate the electron-phonon coupling strength in a binary alloy. For the electron density which determines the Fermi energy, Fermi wave vector and density of states, we have used the average density of the system. Similar averaging is used for the atomic mass M .

In Table I, the quantities $2k_F$, ρ calculated from $A(K)$ corrected from the liquid state and the Animalu-Henle pseudopotential, and the experimental values of ρ are listed. It can be seen that the values of ρ determined from the Ziman theory are in reasonable agreement with the experimental values. We have also determined $L(q)$ for both the l and t modes given in (7) up to $q = 3 \text{ \AA}^{-1}$. The curves for two alloys $\text{Pb}_{90}\text{Cu}_{10}$ and $\text{Tl}(+\text{Te})$ are shown in Fig. 1(a). Those for $\text{In}_{80}\text{Sb}_{20}$ and $\text{Sn}_{90}\text{Cu}_{10}$ look similar and are not included. The values of $L_t(q)$ are normalized to $L(0)$. In Fig. 1(b) are plotted the functions $L(q)$ defined by $L(q) = \frac{1}{3}[L_l(q) + 2L_t(q)]$ for all four alloys. The $N(q)$ curve for $\text{Pb}_{90}\text{Cu}_{10}$ is also included. The purpose of plotting $L(q)$ will be clear in our later discussions. The positions of q_D (so called "equivalent" Debye wave vector determined from total number of modes consideration) are marked on the curves. It can be seen $L(q)$ is a monotonic increasing function of q . This point will be discussed in relation to short-range ordering in the amorphous state. The asymptotic values $L(\infty)/L(0)$ are also listed in Table I to illustrate the variation of $L(q)$ over a large range of q . These results of $L(q)$ and $N(q)$ will be utilized to study the phonon spectrum $F(\omega)$ in Sec. III.

TABLE I. Values of $2k_F$, ρ_{calc} , ρ_{expt} , and $L(\infty)/L(0)$ for four amorphous alloys. We have used the structure factors corrected from the liquid state of In, Sn, Tl by H Hendus, Z. Naturforsch. A2, 505 (1947), and of Pb by P.C. Sharrach and G.P. Smith, J. Chem. Phys. 21, 228 (1953). The resistivity data are taken from Ref. 1.

| Alloys | $2k_F$ (\AA^{-1}) | ρ_{calc} ($\mu\Omega$ cm) | ρ_{expt} ($\mu\Omega$ cm) | $L(\infty)/L(0)$ |
|--------------------------------|------------------------------|--|--|------------------|
| $\text{In}_{80}\text{Sb}_{20}$ | 3.17 | 46 | 33 | 2.27 |
| $\text{Sn}_{90}\text{Cu}_{10}$ | 3.20 | 48 | 47 | 2.12 |
| $\text{Pb}_{90}\text{Cu}_{10}$ | 3.06 | 68 | 78 | 2.36 |
| $\text{Tl}(+\text{Te})$ | 2.92 | 64 | 73 (liquid) | 2.89 |

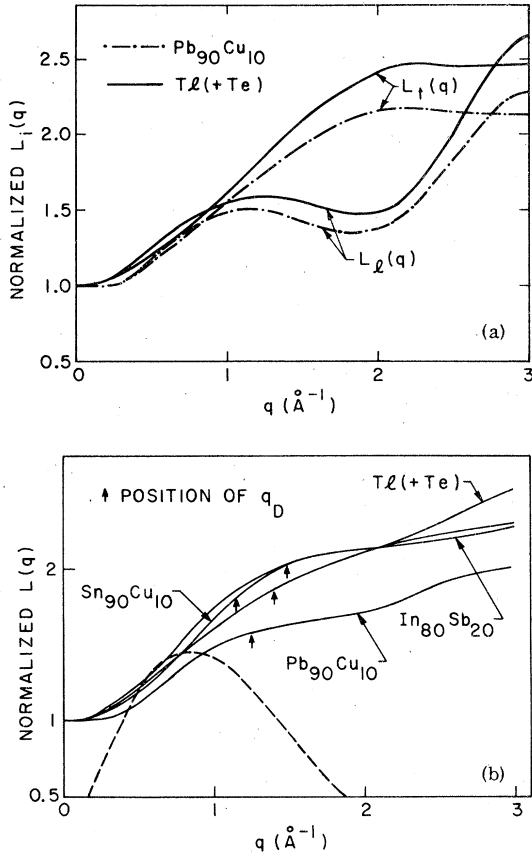


FIG. 1. (a) Normalized $L_i(q)$ vs q for amorphous $\text{Pb}_{90}\text{Cu}_{10}$ and $\text{Tl}(+\text{Te})$ alloys. (b) Normalized $L(q)$ (solid curves) vs q for four amorphous alloys. The positions of the "equivalent" Debye wave vector are marked on the curves. Similar plot of $N(q)$ (dashed curve) for $\text{Pb}_{90}\text{Cu}_{10}$ is also included.

C. Comparison with experiment

In this Section, we shall check our expression of $\alpha^2 F(\omega)$ at least for the low- ω region by going through some numerology. It should be remarked that the region of linearity of $\alpha^2 F(\omega)$ is rather small. This depends on the region of constancy of $L(q)/L(0)$ at low q . Referring to Fig. 1, one notes that this region is $\sim 0.1-0.2 \text{ \AA}^{-1}$ which corresponds to $\lesssim 1 \text{ meV}$ on the energy axis. While if one starts to "crystallize" the amorphous phase fictitiously by introducing perturbation to the structure factor $A(K)$, the region of linearity is reduced or even removed. If an experiment is done by using the $A(K)$ of a "microcrystal" taken from Ref. 16 in the integral $L_i(q)$, then it is found that $L_i(q)/L(0)$ starts at some power law of q at $q=0$ which removes the linear region. However, $\alpha^2 F(\omega)$ is still enhanced with respect to the crystalline values in the low- ω region.

Putting (8) in (6) and performing the integral

over q space at low- ω so that $\omega = vq$, where v is the speed of sound one obtains

$$\alpha^2 F(\omega) = [e^2 E_F k_F^2 N(0) \rho / 3\pi^3 \langle v^3 \rangle m M] \omega = A \omega. \quad (10)$$

$N(0)$ is in states per eV per atom spin, $\langle v^3 \rangle$ is given by $1/\langle v^3 \rangle = (\frac{1}{3}) \times (1/v_l^3 + 2/v_t^3)$, where l and t denote the longitudinal branch and transverse branch, respectively. In an isotropic model $\langle v^3 \rangle$ is also related to the Debye temperature Θ_D by $\Theta_D^3 \propto D \langle v^3 \rangle / M$, where D is the density of the solid. The proportionality constant is determined by knowing Θ_D and $\langle v^3 \rangle$ in amorphous $\text{Pb}(\text{+Bi})$ alloys²³ since $\langle v^3 \rangle \approx v_t^3$ and there is a 15% reduction in transverse velocity of the amorphous phase.²⁴ For alloys where information on Θ_D is lacking, we use the relation $\Theta_D \propto \langle \omega \rangle = \int_0^\infty \alpha^2 F d\omega / \int_0^\infty (\alpha^2 F / \omega) d\omega$ determined from tunneling experiments.¹³ In Table II the theoretical and experimental are listed values of A , the first derivative of $\alpha^2 F(\omega)$ at low ω for seven amorphous alloys and elements. The experimental values of A are taken from Refs. 25-29. The "Remark" column indicates whether $\langle v^3 \rangle$ is determined from Θ_D or $\langle \omega \rangle$ and gives the source of information. Values of ρ are taken from experiments. E_F , k_F , and $N(0)$ are determined from the free-electron model. It can be seen that the present results explain rather well the experimental observations. In fact, we shall use the experimental slope A to generate values of $\langle v^3 \rangle$ for the phonon dispersion curves in Sec. III. The latter requires a higher degree of accuracy.

III. RELATIONSHIP BETWEEN ABSENCE OF STRUCTURAL LONG-RANGE ORDER, PHONON SPECTRUM $F(\omega)$, ATOMIC PARAMETER η , AND TRANSITION TEMPERATURE T_c

In this section, we attempt to deconvolute the phonon spectrum $F(\omega)$ using relation (6)

TABLE II. Comparison of experimental and theoretical values of first derivative of $\alpha^2 F(\omega)$ at low (ω). References on Θ_D and $\langle \omega \rangle$ are also included.

| Alloys | A_{calc} (eV^{-1}) | A_{expt} (eV^{-1}) | Remarks |
|--------------------------------|--|--|--|
| $\text{Pb}_{90}\text{Cu}_{10}$ | 320 | 300 | $\langle \omega \rangle$ (a) |
| $\text{Pb}_{95}\text{Bi}_5$ | 250 | 400 | $\Theta_D \approx 70 \text{ }^\circ\text{K}$ (b) |
| $\text{Sn}_{90}\text{Cu}_{10}$ | 200 | 150 | $\langle \omega \rangle$ (a) |
| Bi | 1300 | ~ 1000 | Θ_D (c) |
| $\text{Tl}(+\text{Te})$ | 115 | 170 | Θ_D (d) |
| $\text{In}_{80}\text{Sb}_{20}$ | 120 | 175 | Θ_D (e) |
| Ga | 190 | ~ 180 | $\langle \omega \rangle$ (f) |

^aReference 27.

^bS. Ewert, Z. Phys. **267**, 283 (1974).

^cReference 23, the Θ_D is determined for $\text{Bi}_{90}\text{Sb}_{10}$.

^dReference 29.

^eA. Comberg and S. Ewert, Z. Phys. B **25**, 173 (1976).

^fReference 25.

and the $L(q)$ and $N(q)$ curves. First, we demonstrate that it is possible to obtain qualitative information on $F(\omega)$ without employing any ω - \vec{q} relation. The argument is rather simple but it offers a preliminary insight into the feature of the phonon modes. For all values of \vec{q} , the l modes are governed by $[L_l(\vec{q}) + N(\vec{q})]/L(0) \leq 3$ and the t modes by $L_t(\vec{q})/L(0) \leq L(\infty)/L(0)$ from Fig. 1. From (6a) we obtain the inequalities $L(0)F(\omega)/\omega \leq \alpha^2 F(\omega) \leq 3L(0)F(\omega)/\omega$ for the l modes and $L(0)F(\omega)/\omega \leq \alpha^2 F(\omega) \leq L(\infty)F(\omega)/\omega$ for the t modes, since $\sum_q \delta(\omega - \omega_q)/\omega_q = F(\omega)/\omega$. The results can be rewritten, for the l modes,

$$\omega \alpha^2 F(\omega)/3L(0) \leq F(\omega) \leq \omega \alpha^2 F(\omega)/L(0), \quad (11a)$$

and for the t modes,

$$\omega \alpha^2 F(\omega)/L(\infty) \leq F(\omega) \leq \omega \alpha^2 F(\omega)/L(0). \quad (11b)$$

The right-hand side comes from the $q=0$ region while the left-hand side comes from the high q region. For a typical $\alpha^2 F(\omega)$ spectrum of an amorphous superconductor, the ratio of the longitudinal mode ω_l to the transverse mode ω_t is ≥ 3 . In any attempt to wash out the features in the l modes, one would pick the $q \approx 0$ result for the t phonons and the high q result for the l phonons in (11). However, one finds that the l peak is still as pronounced as that manifested in the $\alpha^2 F(\omega)$ spectrum from the fact that $\omega_l/\omega_t \geq 3$. It is clear that $q \neq 0$ for all ω_q in the t branch which reduces the t peak even more. Hence the l modes are almost as distinct as the t modes in the phonon spectrum. The strong enhancement of $\alpha^2 F(\omega)$ at the t mode can be understood as coming from the $1/\omega$ dependence of the electron-phonon coupling strength at low ω . Recent theoretical calculations^{7,8} of $F(\omega)$ in model amorphous metals give a single broad band without distinct mode features. It might be that in the first-principles calculations of a model tight-binding amorphous metal the proper short-range order has not been taken into account so that discrepancies exist between experiments and theories. Alternatively, the vibrational spectrum of a d -band metal may be different from that of a simple metal. Weaire *et al.*⁹ have investigated the elastic properties of amorphous metals using the approximation of pairwise central interatomic potentials fitted from experimental data on crystalline materials. By including internal displacements of the atoms in the amorphous structure, that is the structure is allowed to relax to minimize the potential energy, they found a considerable decrease in the shear modulus ($\approx 33\%$) with respect to the corresponding crystalline case. However both the bulk modulus and the density decrease only slightly

($\approx 2\%$ – 3%). These results are in broad agreement with experimental measurements on Ni-P and Pd-Si alloys. On the other hand, using the dense random packing of hard-spheres model produced appreciable softening of both moduli.

In a simplest approach, we have used the quadratic ω_q dispersion curve to deconvolute $F(\omega)$ from $\alpha^2 F(\omega)$. For crystalline s - p metals, Allen³⁰ has used quadratic phonon dispersion curves to evaluate the electron-phonon mass enhancement $\lambda = 2 \int_0^\infty (\alpha^2 F/\omega) d\omega$. The dispersion curves can be generated if one knows (v_t, v_l) and (ω_t, ω_l) . For quadratic dispersion, $v_t/v_l = \omega_t/\omega_l$. The latter pairs are taken from the peaks in the $\alpha^2 F(\omega)$ spectrum. By also knowing $\langle v^3 \rangle$ from the initial slope A in Sec. II C, one can determine v_t and v_l separately. For a given ω in each branch, we find the value of q such that $\omega_q = \omega$ and locate the corresponding value of $L_t(q)$ and $N(q)$ in Fig. 1 so that $N(q) = \tilde{N}(\omega)$ and $L_t(q) = \tilde{L}_t(\omega)$. Then, for each branch we determine $\alpha_i^2(\omega)$ from Eq. (6). The values of α_i^2 are expressed in units of $L(0)$ so that they have the unit $L(0)$ per meV. To determine the phonon spectrum, one needs to know $\langle \alpha^2 \rangle = \alpha^2 F(\omega)/F(\omega)$. The quantity $\langle \alpha^2 \rangle$ is given by $\langle \alpha^2 \rangle = \alpha_l^2 [F_l(\omega)/F(\omega)] + \alpha_t^2 [F_t(\omega)/F(\omega)]$ with $F_i(\omega)/F(\omega) \approx v_i^3/(v_l^3 + v_t^3)$ in the Debye approximation. The values of $\langle \alpha^2 \rangle$ for $\text{Pb}_{90}\text{Cu}_{10}$ thus determined are shown in Fig. 2. The shaded region is obtained by including an uncertainty $\Delta q = \pm \frac{1}{2}q$ for each \vec{q} . For $\omega > \omega_l$ one can use the high q values of $L(q)$ ($q_D < q < 2q_D$). One observes the dominance of the $1/\omega$ term in the low- ω region. A similar procedure is also carried out for the other three alloys. The phonon spectra $F(\omega) = \alpha^2 F(\omega)/\langle \alpha^2 \rangle$ so determined are shown in Fig. 3 together with those obtained for the crystalline phases taken from Ref. 5. The

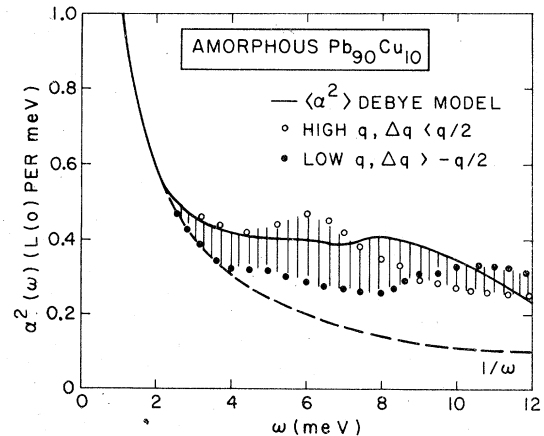


FIG. 2. $\langle \alpha^2 \rangle$ vs ω for amorphous $\text{Pb}_{90}\text{Cu}_{10}$. The $1/\omega$ line is included for comparison. Shaded region represents uncertainty in $\langle \alpha^2 \rangle$ due to uncertainty in \vec{q} .

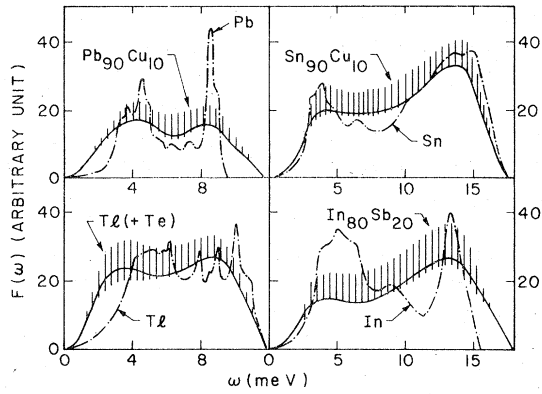


FIG. 3. Phonon spectra (arbitrary unit) for four amorphous alloys and their crystalline counterparts. Shaded regions represent uncertainty in $F(\omega)$ due to uncertainty in \tilde{q} .

curves are not normalized but they are plotted in such a way that the area under amorphous $F(\omega)$ equals that of crystalline phase. The $\alpha^2 F(\omega)$ curves are taken from Refs. 27–29. The shaded regions are obtained by including an uncertainty $\Delta\langle\alpha^2\rangle$ deduced from $\Delta q (= \pm \frac{1}{2}q)$. This uncertainty results from the indeterminacy in \tilde{q} for a given ω in an amorphous solid. However, we believe that such inclusion is not required for the low-lying phonon modes. It should be pointed out that high \tilde{q} ($\sim \tilde{q}_D$) is more favorable for intermediate-to-high energy phonons as will be discussed later.

$$\begin{aligned} \eta_{\text{am}} &= \left(\frac{2M}{\hbar}\right) \int_0^\infty \omega \alpha^2 F(\omega) d\omega \\ &= \left(\frac{2M}{\hbar}\right) \sum_q \int_0^\infty [N(\tilde{q}) + L_i(\tilde{q})] \delta_i(\omega - \omega_q) d\omega + \left(\frac{2M}{\hbar}\right) \sum_q \int_0^\infty L_i(\tilde{q}) \delta_i(\omega - \omega_q) d\omega \\ &= \frac{\eta_{\text{xtal}}}{3} + \left(\frac{\eta_{\text{xtal}}}{3N}\right) \sum_q \int_0^\infty \left[\left(\frac{L_i(\tilde{q})}{L(\infty)}\right) \delta_i(\omega - \omega_q) + \left(\frac{2L_i(\tilde{q})}{L(\infty)}\right) \delta_i(\omega - \omega_q) \right] d\omega. \end{aligned} \quad (12)$$

The last step follows from the fact that $N(\tilde{q})$ only couples to the longitudinal phonons. $L(\infty)$ is given in (9). It should be noted that η so defined for the amorphous phase depends on the phonon spectrum. An absolute upper bound $\eta_{\text{am}} < (\frac{1}{3})\eta_{\text{xtal}}$ is obvious from (12). A more stringent upper bound is obtained by taking $L_i(\tilde{q})$ at the characteristic wave vector \tilde{q}_D . Using the $L_i(q_D)/L(\infty)$ values from Fig. 1, one obtains η_{am} smaller than 0.97, 1.0, 1.1, and 1.2 times of η_{xtal} for amorphous Tl(+Te), $\text{Pb}_{90}\text{Cu}_{10}$, $\text{Sn}_{90}\text{Cu}_{10}$, and $\text{In}_{80}\text{Sb}_{20}$ alloys, respectively. In Table III are listed the values of η in amorphous, highly disordered and crystalline phases of different s - p metals and alloys. It is observed that

The consequence of which is that smaller uncertainty $\Delta L(q)$ is expected for $\omega \gtrsim \omega_t$ (see Fig. 1).

Several features are noted in Fig. 3. Both peaks in the crystalline phases are broadened appreciably in the amorphous phase. However, the smearing occurs almost equally in the low- and high- ω regions with the longitudinal modes persisting in the amorphous phase. Comparing the phonon moments such as $\int_0^\infty \omega F(\omega) d\omega$ and $\int_0^\infty [F(\omega)/\omega] d\omega$ in the two phases, one does not observe a significant change due to phase transformation. This conclusion is in better agreement with theoretical results^{7,8} obtained using the Morse potential than the Lennard-Jones potential. The latter indicates a significant shifting of the characteristic modes to lower energy. In fact, Bolz and Pöbel¹⁰ observed almost the same value of $\int_0^\infty [F(\omega)/\omega] d\omega$ in both crystalline and amorphous Sn. On the other hand, one expects quite a significant change of these two moments obtained from $\alpha^2 F(\omega)$. The dominance of the $1/\omega$ term in $\langle\alpha^2\rangle$ highly enhances the low- ω contribution.

Another interesting property which results from the monotonic behavior of $L(q)$ is that the Hopfield-McMillan atomic parameter η tends to decrease in the amorphous phase. This is based on the assumption that there is no significant change in the pseudopotential form factor V_Q associated with the phase transformation. η_{am} is defined in the usual way as

the above inequalities are obeyed and that there is a general trend for η to decrease in the amorphous state. This point was first noted by Allen and Dynes.³¹ The fact that good agreement is reached by taking $L(\tilde{q})$ at the characteristic wave vector \tilde{q}_D suggests that the intermediate-to-high energy phonons are better described by large wave vectors.

Mathematically, the decrease in $L(q)$ at low q originates from the particular form of $A(K)$ for an amorphous structure. In Fig. 4(a) is shown the graph of a typical structure factor in which the positions of $2k_F$ for metals of different valencies z are marked. Since the factor $Q^3 V_Q^2$ of the

TABLE III. Values of the Hopfield-McMillan atomic parameter η (eV \AA^{-2}) for *c* (crystalline), *d* (disordered), and *a* (amorphous) superconductors.

| | | | |
|--------------------|---|---|--------------------|
| <i>c</i> -Pb (2.4) | <i>d</i> -Pb (2.24) | <i>a</i> -Pb ₉₀ Cu ₁₀ (1.8) | <i>a</i> -Pb (2.0) |
| <i>c</i> -Sn (2.2) | <i>d</i> -Sn (2.1) | <i>a</i> -Sn ₉₀ Cu ₁₀ (1.5) | |
| <i>c</i> -Tl (1.2) | <i>a</i> -Tl (1.1) | | |
| <i>c</i> -In (1.3) | <i>d</i> -In ₈₀ Sb ₂₀ (1.3) | <i>a</i> -In ₈₀ Sb ₂₀ (1.4) | |
| β -Ga (2.0) | <i>a</i> -Ga (2.1) | | |

integrand $A(Q)Q^3V_Q^2$ of $L(0)$ has appreciable contributions in the region where $A(Q)$ is small, the intermediate Q (or equivalently the intermediate range) portion of the electron-ion interaction $Q^3V_Q^2$ is attenuated. The loss of periodicity apparently leads to a partial "destructive interference" in the electron-ion interaction. Even from a structural point of view, the sharp peak in $A(K)$ does originate from the periodic oscillation in the reduced radial-distribution function $G(r) = 4\pi r[\rho(r) - \rho_0]$ which is characteristic of the loss of long-range order in a solid. In Fig. 4(b) is shown a typical graph of $G(r)$. The dotted line in Fig. 4(b) is a Fourier transform fitting of the dashed line in Fig. 4(a) for amorphous Ni-P alloys¹⁶ illustrating the correlation between the first peak in $A(K)$ and the loss of long-range ordering. By increasing q , there is a tendency to move $Q^3V_Q^2$ away from the low- Q region and thus $L(q)$ is enhanced. Physically, the high- q phonons do not "see" the structural disorder since they are more or less localized to interatomic distances. While at intermediate q , the long-range disorder is well scanned. Lastly, it should be men-

tioned that the above discussion is valid only when $Q^3V_Q^2$ has significant contribution at low-to-intermediate Q , such as in the case of *s-p* metals. However, in transition metals $Q^3V_Q^2$ has the most important contribution around $2k_F$ and equals ≈ 0 for $q \leq 2k_F$ typical of *d* resonance. In that case, the short-range character of $A(K)$ is fully utilized. This will be discussed in detail in our future work.

We have not succeeded in finding a rigorous correlation between the enhancement in the electron-phonon coupling constant λ and its effect on the transition temperature T_c . However, several points we observed deserve mentioning. The detailed analysis of T_c for strong-coupled superconductors was due to Allen and Dynes.³¹ They included thermal phonons (pair breakers) effect in their self-consistent solution of the Eliashberg equation. The consequence is that it is more difficult to enhance T_c in soft materials than one would expect at first sight. It was found that T_c is related to the different moments of $\alpha^2F(\omega)$ in a sophisticated way. From Fig. 10 of their work, one observes a general trend between T_c/ω_{10g} and λ . An enhancement in λ certainly increases the ratio T_c/ω_{10g} but it does not imply an increase in T_c since ω_{10g} decreases. We can compare the two cases (i) Pb versus amorphous Pb₉₀Cu₁₀, and (ii) Sn versus amorphous Sn₉₀Cu₁₀.²⁷ In (i), λ increases from 1.66 in Pb to 2.0 in Pb₉₀Cu₁₀, T_c/ω_{10g} increases from 0.15 to 0.18. However, $\omega_{10g} \approx \langle \omega^2 \rangle^{1/2} = (\eta/\lambda M)^{1/2}$ decreases by $\sim 22\%$ which causes an overall decrease in T_c by $\sim 0.5^\circ\text{K}$. In case (ii), λ increases from 0.7 in Sn to 1.82 in Sn₉₀Cu₁₀ and η decreases from 2.2 to 1.5 eV/\AA^2 , T_c/ω_{10g} increases by a factor of 4. On the other hand, ω_{10g} decreases by a factor of 2 which still maintains an overall increase in T_c by $\sim 3.6^\circ\text{K}$. The thermal phonons effect leads to a decreased increment in T_c/ω_{10g} per unit λ for $\lambda > 2$. Thus, a small decrease in η is sufficient to nullify the effect of enhanced λ in the high λ region. Given the fact that λ cannot be too large (say, ≤ 3) as limited by lattice instability, the change in T_c would depend strongly on the initial λ in the crystalline phase. The latter sets a range over which λ can be further increased.

The last point we discuss in this section is the

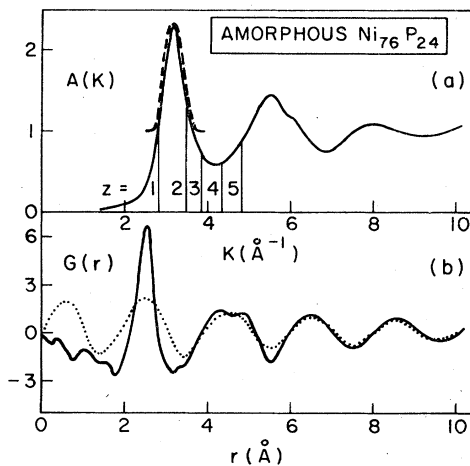


FIG. 4. (a) Structure factor $A(K)$ and (b) reduced radial distribution function $G(r)$ for amorphous Ni₇₆P₂₄ alloys (Ref. 16). Positions of $2k_F$ for different valences are marked on $A(K)$. The dotted line in (b) is a Fourier transform fitting of the dashed line in (a).

relationship between amorphousness and the strong-coupling criterion. By using McMillan's criterion, the crossover point from weak coupling to strong coupling occurs at $\lambda \approx 1$. An "equivalent" criterion is the positive deviation from the BCS gap coefficient $2\Delta_0/k_B T_c$. It should be noted that some of the superconductors considered here are already strong coupling in the crystalline phase. It was found that amorphous *s-p* superconductors are mostly strong coupling. One can understand this property by considering the increment $\delta\lambda$ due to phase transformation. In the crystalline phase $\alpha^2 F(\omega)$ is small while in the amorphous phase $\alpha^2 F(\omega) \approx A\omega$ for $\omega \lesssim 1-2$ meV. From Sec. II C, $A \geq 150-1000$ eV⁻¹ and thus $\delta\lambda \geq 0.6-1$ (we have used the experimental values of A to obtain the range of $\delta\lambda$). Such increments can easily bring λ above one in the amorphous phase. On the contrary, it was found that amorphous transition-metal alloys are weak coupling.³² From (10), $A \propto k_F^2 E_F N(0) \rho D / M^2 \Theta_D^3$, the factor $M^2 \Theta_D^3 / E_F k_F^2$ ($\Theta_D \approx 250$ °K estimated from $T_c \approx 8$ °K for amorphous Mo, $M \approx 100$ amu, $E_F \approx 5$ eV) is ~ 30 times its corresponding value in *s-p* metals ($\Theta_D \approx 60$ °K). Therefore, A is still decreased by a factor of ~ 2 despite an increase in $DN(0)\rho$ and thus the enhancement $\delta\lambda$ is suppressed.

IV. COMPARISON STUDY: $\alpha^2 F(\omega)$ IN CRYSTALLINE Pb

In order to compare the features of electron-phonon interacting in the amorphous and crystalline phases, a simple calculation along the line of Sec. II is done for crystalline Pb. $\alpha^2 F(\omega)$ is derived based on the assumptions of isotropic Fermi surface and phonon spectrum, and free-electron matrix elements. An additional assumption of a Debye sphere for the phonon Brillouin zone allows the evaluation of $\langle \alpha^2 \rangle$. There had been calculations of λ for simple metals using a similar set of assumptions.³⁰ It was concluded that results on metals like Al and Pb with the fcc structures, well-known phonon spectra, and rather free-electron-like Fermi surfaces were in good agreement with experiments. To obtain the fine structure in $\alpha^2 F(\omega)$ in addition to the two main peaks, more sophisticated calculations are required, such as those performed by Carbotte³³ for crystalline Tl. Carbotte obtained the phonon energy ω_q for $g_{k',k,q}$ by fitting neutron-scattering data to the Born-von Kármán force-constant model. However, for our purpose of qualitative comparison at the present, a simplified calculation of $\alpha^2 F(\omega)$ is sufficient.

The condition $\vec{k}' - \vec{k} + \vec{q} = 0$ or \vec{G} with both \vec{k} and \vec{k}' lying on the Fermi surface allows us to write $\alpha^2 F(\omega)$ in the form of (6a) with $L(\vec{q})$ of (6b) now

given by

$$L(\vec{q}) = \frac{\pi^2 \hbar N(0)}{6Mk_F^2} \sum_{\vec{G} \neq 0} \frac{|\vec{\epsilon}_q \cdot (\vec{q} + \vec{G})|^2 V_{\vec{q}+\vec{G}}^2}{|\vec{q} + \vec{G}|} \times H(2k_F - |\vec{q} + \vec{G}|), \quad (13)$$

where H is the Heaviside step function which results from the condition $|\vec{k}' - \vec{k}| \leq 2k_F$, the factor $|\vec{q} + \vec{G}|$ in the denominator comes from restricting the final states \vec{k}' to the Fermi surface. To simplify further, we assume that the polarization vectors $\vec{\epsilon}_q$ are purely longitudinal ($\vec{\epsilon}_q \parallel \vec{q}$) for transverse ($\vec{\epsilon}_q \perp \vec{q}$). Thus, the N process will be purely longitudinal. We also assume an isotropic phonon spectrum so that $L(\vec{q}) = L(q)$ and rewrite $L(q)$ as

$$L(q) = U_l(q) + U_t(q). \quad (14)$$

The first term represents the l contribution and the last term represents the t contribution to the U process. The latter results from averaging $|\vec{\epsilon}_q \cdot \vec{G}|$ over orientations of $\vec{\epsilon}_q$ perpendicular to \vec{q} . We have also used the Heine-Animalu pseudopotential form factor for $V_{\vec{q}+\vec{G}}$. The computer results of $U_l(q) + N(q)$ and $U_t(q)$ for crystalline Pb are shown in Fig. 5. $\langle \alpha^2 \rangle$ is then obtained by the procedure described in the last section and is shown in Fig. 6. The arrows indicate the l and t peaks in the $\alpha^2 F(\omega)$ spectrum. It is seen that in the region of interest $2 < \omega < 9$ meV, $\langle \alpha^2 \rangle$ deviates significantly from the $1/\omega$ line. The slow variation of $\langle \alpha^2 \rangle$ as a function of ω implies a close similarity between $F(\omega)$ and $\alpha^2 F(\omega)$ in crystalline Pb. In fact, this latter feature might even be more gen-

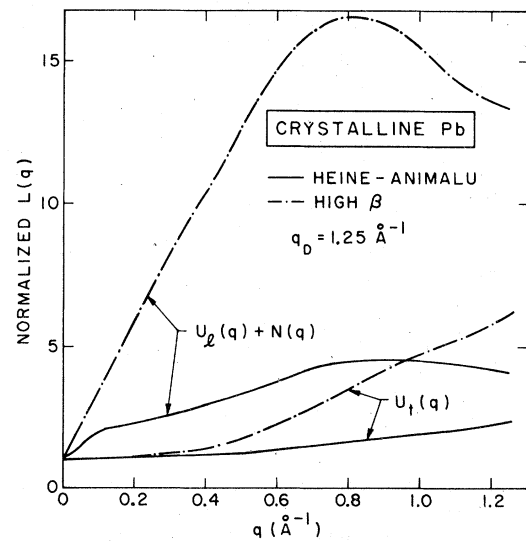


FIG. 5. $U_l(q) + N(q)$ and $U_t(q)$ vs q evaluated for the Heine-Animalu and high- β pseudopotentials (Ref. 20).

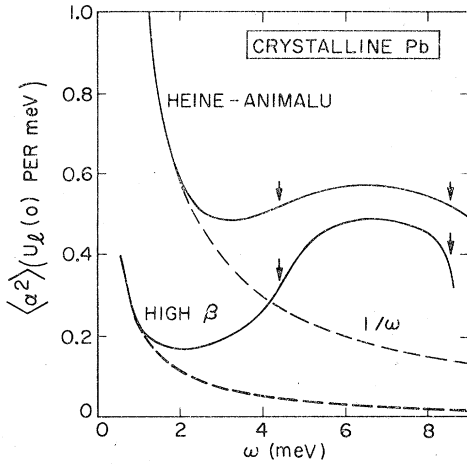


FIG. 6. $\langle \alpha^2 \rangle$ vs ω for the Heine-Animalu and high- β pseudopotentials. All values are normalized to $U_l(0)$ determined for the Heine-Animalu case. The $1/\omega$ line is included for comparison.

eral than the present result would imply.⁵ One also observes from Fig. 5 that $\langle \alpha^2 \rangle$ tends to diverge at $\omega < 2$ meV. However, a careful consideration shows that such a divergence is fortuitous. The faults are in the choice of model pseudopotentials and the use of single orthogonal plane waves in our calculation. It is found that the low- ω results are very sensitive to the choice of pseudopotentials since the values of V_{G_0} (\vec{G}_0 are those reciprocal lattice vectors which satisfy $|\vec{G}| < 2k_F$) determines $\tilde{L}(\omega)$ in the low- ω region. On the contrary, such sensitive dependences on the pseudopotentials are not found in the amorphous case. For example, we have repeated our calculation by using the high- β pseudopotential²⁰ which is supposed to be more realistic than the Heine-Animalu pseudopotential for crystalline Pb. The results are included in Figs. 5 and 6. It can be seen that the divergence is highly attenuated even at $\omega < 1$ meV. Despite a larger overall variation in $\langle \alpha^2 \rangle$, the couplings are almost equal for both l and t modes.

V. SUMMARY AND CONCLUSION

We have derived a simple expression of the Eliashberg function of $\alpha^2 F(\omega)$ for an amorphous s - p superconductor using the pseudopotential theory. The expression depends on the phonon energy ω_q , the structure factor $A(K)$ of the amorphous phase, and the pseudopotential form factor $v_{kk'}$. The loss in translational symmetry introduces a new set of selection rules for \vec{k} , \vec{k}' , and \vec{q} through $A(K)$, where $K = |\vec{k}' - \vec{k} + \vec{q}|$. For $\vec{q} \approx 0$, the range of K ($K \leq 2k_F$ but not necessarily equal to \vec{G}) for which $A(K) > 0$ yields a contribution to the electron-phonon coupling due to nonconserva-

tion of lattice momentum in the conventional sense. This range depends on the valence z as can be seen in Fig. 4. For the high valence materials ($z \geq 3$), it contributes to a rather appreciable value of $L(0)$. The range of \vec{q} over which $L(\vec{q})$ is constant then yields a linear dependence of $\alpha^2 F(\omega)$ on ω in the low-energy region. We find that the ω dependence of $\alpha^2 F(\omega)$ in this region is sensitive to the degree of disorder. The result is found to agree well with tunneling experiments. We have attempted to deconvolute the phonon spectrum $F(\omega)$ from $\alpha^2 F(\omega)$ using the quadratic phonon-dispersion relation and also taking into account the uncertainties in \vec{q} for a given ω in the amorphous phase. The results indicate the dominance of the $1/\omega$ term in $\langle \alpha^2 \rangle$ in the low- ω region. There is no appreciable change in the first moment and first inverse moment of $F(\omega)$ due to phase transformation despite an appreciable smearing in the phonon density of states. The longitudinal modes are still distinctly separated from the transverse modes. These observations suggest that any first-principles calculation of $F(\omega)$ should take into account a more realistic short-range order in the amorphous phase. The present results should also be checked by performing neutron scattering experiments on amorphous metals. We have correlated the absence of long-range order and a general suppression of the Hopfield-McMillan atomic parameter η (which depends on the phonon spectrum) in amorphous superconductors. However, we have not succeeded in deriving a rigorous relationship between δT_c , $\delta \lambda$, and $\delta \eta$. The effect of amorphousness on the strong-coupling behavior is discussed. We have also performed a similar calculation for crystalline Pb. It is found that $\langle \alpha^2 \rangle$ weights almost equally on both l and t phonons. The feature in the low- ω region is observed to depend sensitively on the choice of pseudopotentials.

ACKNOWLEDGMENTS

The authors thank S. Swartztrauber for assistance with the numerical calculations. One of us (S.J.P.) acknowledges Professor W. A. Harrison for discussions on the perturbation theory in amorphous and liquid metals. Gratitude is also extended to Professor M. R. Beasley for bringing Ref. 17 to the authors attention. This work was supported by the Air Force Office of Scientific Research (AFSC), United States Air Force.

APPENDIX

The first-order matrix element of the electron-phonon interaction has been evaluated in Sec. IIA

using a free-electron model. Here we estimate the corrections due to the second-order term. The electron-ion scattering matrix element calculated to second order is given by²⁰

$$\langle k' | \bar{v} | k \rangle = \langle k' | v | k \rangle + \sum_{k''} \frac{\langle k' | v | k'' \rangle \langle k'' | v | k \rangle}{(\hbar^2/2m)(k^2 - k''^2)}, \quad (\text{A1})$$

where $v = (1/N) \sum_i v(\vec{r} - \vec{R}_i - \vec{u}_i)$, \vec{u}_i is the atomic displacement. Writing $v(\vec{r} - \vec{R}_i - \vec{u}_i)$ as $v(\vec{r} - \vec{R}_i) + \vec{u}_i \cdot \nabla v$ in (A1) and retaining terms up to \vec{u}_i , we obtain

$$\begin{aligned} \langle k' | v | k'' \rangle \langle k'' | v | k \rangle &= \sum_i B_{k'k''i} \sum_m B_{k''km} \\ &+ \sum_m B_{k''km} \sum_i B_{k'k''i} \vec{u}_i \cdot (\vec{k}' - \vec{k}'') \\ &+ \sum_i B_{k'k''i} \sum_m B_{k''km} \vec{u}_m \cdot (\vec{k}'' - \vec{k}), \end{aligned} \quad (\text{A2})$$

where $B_{k'k''i} = v_{k'k''i} \exp[i(\vec{k}' - \vec{k}'') \cdot \vec{R}_i]$ and $v_{k'k''i}$ is the pseudopotential form factor.

The last two terms in (A2) corresponds to higher-order "structural" correction to the electron-phonon matrix element. Taking a positional average on \vec{u}_i , these correction terms give

$$\begin{aligned} \sum_m B_{k''km} \sum_i B_{k'k''i} \langle \vec{u}_i \cdot (\vec{k}' - \vec{k}) \rangle \\ \approx v_{k'k''} [A(|\vec{k}' - \vec{k}''|)]^{1/2} \\ \times v_{k'k''} [A(|\vec{k}'' - \vec{k}|)]^{1/2} \langle \vec{u}_i \cdot (\vec{k}' - \vec{k}) \rangle, \end{aligned} \quad (\text{A3})$$

since

$$A(K) = \frac{1}{N} \left(\sum_i e^{i\vec{K} \cdot \vec{R}_i} \right)^2$$

and

$$\sum_i e^{i\vec{K} \cdot \vec{R}_i} = \int_0^\infty 4\pi R^2 \rho(R) \left(\frac{\sin KR}{KR} \right) dR = \text{real}.$$

Using the pseudopotential form factor and the amorphous structure factor, one notices that $v_k[A(K)]^{1/2} \rightarrow 0$ at low K and it reaches a plateau value of ~ 1 eV at intermediate K . At $K \gtrsim 2k_F$, it approaches zero as $1/K^2$. This has been checked for several simple metals of interest. Thus, one can use a square-well model of the form

$$v_k[A(K)]^{1/2} = \begin{cases} E_0, & K < 2k_F, \\ 0, & K > 2k_F. \end{cases} \quad (\text{A4})$$

Using (A4) in the correction term, one obtains

$$\begin{aligned} \sum_{k''} \frac{\langle k' | v | k'' \rangle \langle k'' | v | k \rangle}{(\hbar^2/2m)(k^2 - k''^2)} \\ \approx \left(\frac{3\pi^2}{4k_F^3} \right) \sum_{k''}^{2k_F} \frac{E_0^2 \langle \vec{u}_i \cdot (\vec{k}' - \vec{k}) \rangle}{(\hbar^2/2m)(k^2 - k''^2)} + \dots + \dots, \end{aligned} \quad (\text{A5})$$

where the dots stand for second-order non-phonon terms and for terms higher in order than E_0^2 . The factor $(3\pi^2/4k_F^3)$ comes from the normalization condition $\sum_{k''} |k''\rangle \langle k''| = 1$. The summation in (A5) can be easily shown to be

$$\left(\frac{3\pi^2}{4k_F^3} \right) \left(\frac{2E_0^2}{\hbar^2} \right) \frac{4\pi}{(2\pi)^3} \int_0^{2k_F} \frac{k''^2 dk''}{k^2 - k''^2} \approx \frac{E_0^2}{E_F}. \quad (\text{A6})$$

Hence, the ratio of second-order term to first-order term for electron-phonon interaction is $\sim E_0/E_F$. With $E_0 \sim 1$ eV and $E_F \sim 10$ eV for simple metals, one sees that the correction term is an order of magnitude less than the original term we derived in Sec. IIA.

¹G. Bergmann, Phys. Lett. C **27**, 159 (1976), and references on specific-heat experiments cited below.
²G. M. Eliashberg, Zh. Eksp. Teor. Fiz. **38**, 966 (1960); **39**, 1437 (1960) [Sov. Phys.-JETP **11**, 696 (1960); **12**, 1000 (1961)].
³J. R. Schrieffer, *Theory of Superconductivity* (Benjamin, New York, 1964).
⁴G. Bergmann, Phys. Rev. B **3**, 3797 (1971).
⁵J. M. Rowell and R. C. Dynes, in *Phonons*, edited by M. A. Nusimovici (Flammarion, Paris, 1971), p. 150 and references cited therein.
⁶L. V. Heimendahl, M. F. Thorpe, and R. Alben, International Conference on Electronic and Magnetic Properties of Liquid Metals, Mexico, 1975 (unpublished); L. V. Heimendahl and M. F. Thorpe, J. Phys. F **5**, L87 (1975).
⁷A. Rahman, M. J. Mandell, and J. P. McTague, J. Chem. Phys. **64**, 1564 (1976).
⁸J. J. Rehr and R. Alben, Phys. Rev. B **16**, 2400 (1977), and references cited therein.

⁹D. Weaire, M. F. Ashby, J. Logan, and M. J. Weins, Acta Metall. **19**, 779 (1971). This is a theoretical paper but see the experimental results cited therein.
¹⁰J. Bolz and F. Pobell, Z. Phys. B **20**, 95 (1971).
¹¹J. Hubbard and J. L. Beeby, J. Phys. C **2**, 556 (1969).
¹²G. Busch and H.-J. Güntherodt, *Solid State Physics*, edited by H. Ehrenreich, F. Seitz, and D. Turnbull (Academic, New York-London, 1974), Vol. 29, p. 235.
¹³W. L. McMillan, Phys. Rev. B **167**, 331 (1968).
¹⁴P. B. Allen, Phys. Rev. B **6**, 2577 (1972).
¹⁵See, for example, J. M. Ziman, *Electrons and Phonons* (Oxford U. P., London, 1960), p. 182. We have written the atomic displacement operator $\delta\vec{R}_i$ as $\delta\vec{R}_i = \sum_q (\hbar/2MNv\omega_q)^{1/2} e^{i\vec{q} \cdot \vec{R}_i} \cdot \epsilon_q (a_q^+ + a_{-q})$.
¹⁶G. S. Cargill III, *Solid State Physics*, edited by H. Ehrenreich, et al., (Academic, New York-London, 1975), Vol. 30, p. 227.
¹⁷Bruno Keck and Albert Schmid, J. Low Temp. Phys. **24**, 611 (1976), and references cited therein.
¹⁸J. M. Ziman, Philos. Mag. **6**, 1013 (1961).

- ¹⁹O. Drierach, R. Evans, H.-J. Güntherodt, and H.-V. Kunzi, *J. Phys. F* 2, 709 (1972).
- ²⁰A. O. E. Animalu and V. Heine, *Philos. Mag.* 12, 1249 (1965). Here we have used the tabulated values of V_Q given by W. A. Harrison, *Pseudopotentials in the Theory of Metals* (Benjamin, New York, 1966).
- ²¹P. Andonov, *J. Con-Crystall. Solids* 22, 145 (1976).
- ²²J. K. Percus and G. H. Yevick, *Phys. Rev.* 110, 1 (1958).
- ²³G. Krauss and W. Buckel, *Z. Phys. B* 20, 147 (1975). We have not investigated the role played by those low-lying phonon modes which give a linear T -dependent specific heat on the electron-phonon interaction.
- ²⁴Brage Golding, B. G. Bagley, and F. S. L. Hsu, *Phys. Rev. Lett.* 29, 68 (1972).
- ²⁵T. T. Chen, J. T. Chen, J. D. Leslie, and H. J. T. Smith, *Phys. Rev. Lett.* 22, 526 (1969).
- ²⁶J. E. Jackson, C. V. Briscoe, and H. Wühl, *Physica* (Utr.) 55, 447 (1971).
- ²⁷K. Knorr and N. Barth, *Solid State Commun.* 8, 1085 (1970).
- ²⁸S. Ewert and A. Comberg, *Solid State Commun.* 18, 923 (1976).
- ²⁹S. Ewert and A. Comberg, *Mater. Sci. Eng.* 23, 275 (1976).
- ³⁰P. B. Allen and M. L. Cohen, *Phys. Rev.* 187, 525 (1969), and other references on the calculations of λ for crystalline Pb cited therein.
- ³¹P. B. Allen and R. C. Dynes, *Phys. Rev. B* 12, 905 (1975).
- ³²C. C. Tsuei, W. L. Johnson, R. B. Laibowitz, and J. M. Viggiano, *Solid State Commun.* (to be published).
- ³³J. P. Carbotte, in *Low Temperature Physics—LT13*, edited by K. D. Timmerhaus, W. J. O'Sullivan, and E. F. Hammel (Plenum, New York London, 1974), Vol. 3, p. 587.